

## THE EXOTIC HELIUM VARIABLE PG 1346+082

M. A. WOOD, D. E. WINGET,<sup>1</sup> R. E. NATHER, AND FREDERIC V. HESSMAN

Department of Astronomy and McDonald Observatory, University of Texas at Austin

JAMES LIEBERT<sup>2,3</sup>

Department of Astronomy and Steward Observatory, University of Arizona

DONALD W. KURTZ

Department of Astronomy, University of Cape Town

F. WESEMAEL<sup>3</sup>

Département de Physique, Université de Montréal

AND

G. WEGNER<sup>3,4</sup>

Department of Physics and Astronomy, Dartmouth College

Received 1986 April 14; accepted 1986 August 13

### ABSTRACT

We present an analysis of the blue object PG 1346+082, which is both a photometric and a spectroscopic variable. The system spans the *B* magnitude range 13.6–17.2; archival data reveal that the system is brighter than  $m_{pg} \approx 14.0$  roughly 74% of the time and has a photometric quasi-period of 4–5 days. High-speed photometric data usually show a dominant 1490 s periodicity and harmonics; at maximum light, the pulse shape is nearly saw-toothed, with a steep rise and gentler fall. Rapid flickering is present in the light curve at minimum light. The system also shows spectroscopic variations, displaying broad, shallow He I absorption lines at maximum light, and a weak emission feature at He I  $\lambda 4471$  at minimum light.

We identify the rapid photometric flickering at minimum light as the signature of mass transfer in a binary system, and the He I emission at minimum light as indicating the presence of an accretion disk. The width of the absorption lines near maximum light then arises as the natural consequence of rotational and pressure broadening in an optically thick accretion disk around a compact mass acceptor. Our inability to detect high-energy X-rays, and the absence of the high-excitation lines of He II in the optical spectrum, rule out any object more compact than a white dwarf as the mass acceptor.

The complete absence of hydrogen in the spectrum identifies the mass donor as a compact, helium degenerate star; in order for mass transfer to occur, this object must be less massive and have a larger radius than its companion.

We conclude that PG 1346+082 is an interacting binary white dwarf system—the second such system to be unambiguously identified—and that this identification lends strong support to the interacting twin-degenerate interpretation for AM CVn.

*Subject headings:* stars: binaries— stars: individual — stars: variables — stars: white dwarfs — ultraviolet: spectra

### I. INTRODUCTION

We present the results of an extensive study of the Palomar Green (Green, Schmidt, and Liebert 1986, hereafter PG) survey object PG 1346+082 (Nather 1984; Nather *et al.* 1984) which consists of time series photoelectric and photographic photometry and spectroscopy. We observed the object because of the similarity of its classification spectrum to the spectrum of the peculiar helium variable AM CVn (=HZ 29; Falkner, Flan-

nery, and Warner 1972). Although this object has long been suspected to be an interacting binary white dwarf (IBWD) system, we have so far been unable to prove that this is the only plausible model which can fit the observations (for a recent review, see Solheim *et al.* 1984). The helium variable GP Com (alias G61-29) has, however, been shown to be an interacting twin degenerate system by the detection of the “s-wave” in its optical spectrum, which revealed an orbital period of 2790 s (Nather, Robinson, and Stover 1981).

We discovered that PG 1346+082 is a photometric variable in 1983, using the high-speed photometer on the 2.7 m telescope at McDonald Observatory, and found that the light curve was strikingly similar to that of AM CVn. Since then we have collected a wealth of high-speed photometric data, including extended coverage data obtained in conjunction with the South African Astronomical Observatory (SAAO). We studied the long-time scale, large-amplitude photometric behavior using the archival Harvard Meteor Program (HMP) films in the Harvard Plate Stacks. In addition to the photometric data, we have obtained spectra during the system's high,

<sup>1</sup> Alfred P. Sloan Research Fellow.

<sup>2</sup> Research performed in part using the Multiple Mirror Telescope, operated jointly by the University of Arizona and the Harvard Smithsonian Center for Astrophysics.

<sup>3</sup> Guest Observer with the *International Ultraviolet Explorer Satellite*, which is sponsored and operated by the National Aeronautics and Space Administration, by the Science Research Council of the United Kingdom, and by the European Space Agency.

<sup>4</sup> Visiting Astronomer, Kitt Peak National Observatory, National Optical Astronomy Observatories, which is operated by the Association of Universities for Research in Astronomy, Inc., under contract with the National Science Foundation.

intermediate, and low states, and have also obtained data using the *International Ultraviolet Explorer (IUE) Satellite*.

PG 1346+082 is both a spectroscopic and a photometric variable, and it shows a wide range of curious properties. The object displays only lines of helium in its optical spectrum; it has a blue energy distribution, fitting an estimated temperature of 15,000–25,000 K; its spectral features are broad ( $\sim 100 \text{ \AA}$ ), and vary from shallow absorption to weak emission; it displays photometric variations which are at least quasi-periodic on time scales ranging from 200 s to a few days. These variations are confined to four distinct domains: 200–400 s, 1490 s, 2.83 hr, and 4–5 days. The amplitudes of the three shorter time scale variations are on the order of 1%, while that of the long-time scale variations is roughly 3.5 mag—spanning the  $B$  magnitude range 13.6–17.2. The system is brighter than  $m_{pg} \approx 14.0$  roughly 74% of the time.

In § II we present the photometric observations, including both the photoelectric and photographic data. In § III we present the spectroscopic data and discuss the results of the *IUE* observations. In § IV, we discuss our model of PG 1346+082 and its theoretical implications. Finally, in § V, we speculate on what we may learn from further study of this and similar systems.

## II. PHOTOMETRIC AND PHOTOGRAPHIC ANALYSES

### a) The Observations

The McDonald Observatory photometric data were obtained using a standard high-speed, two-star photometer (Nather 1973) on the 2.7, 2.1, 0.9, and 0.8 m telescopes. We used a blue-sensitive photomultiplier tube with a bialkali photocathode (an RCA 8850). Additional high-speed photometric data obtained by D. W. K. of the University of Cape Town were taken with a single-channel photometer (an EMI 6256 photomultiplier tube) on the 0.9 m telescope at the SAAO.

For the differential photometric measurements, we used a standard Johnson  $UBV$  filter set and 5 s integrations. Our primary standard star was Feige 84, which has colors ( $V = 11.84$ ,  $B - V = -0.17$ ,  $U - B = -0.74$ ) similar to PG 1346+082, and whose position in the sky is only about  $6^\circ$  away. We obtained both “instantaneous” differential magnitudes (i.e., roughly 2 minutes each on the program and standard stars), and differential magnitudes time-averaged over the dominant 1490 s photometric periodicity. In addition, H.G. Corwin (private communication) obtained calibrated  $UBVRI$  measurements during two of our high-speed observing runs. We obtained a total of 24  $UBV$  measurements on 19 nights, the details of which are listed in Table 1.

Our unfiltered high-speed photometric data were obtained as described by Kepler *et al.* (1982). We typically used 10 s integrations while taking the data and later summed them into 30 s bins after determining that there was no power above 1.5 millimagnitudes (mmag) from 20 s to 120 s in any of our amplitude spectra. We have obtained a total of 102.5 hr of high-speed photometric data since 1983 and present the journal of observations in Table 2.

### b) Multicolor Photoelectric Photometry

We find that the  $B$  magnitude of PG 1346+082 varies from  $13.6 \pm 0.09$  to  $17.2 \pm 0.10$ . The system is blue, having mean  $B - V$  and  $U - B$  colors of  $-0.07$  and  $-0.97$ , respectively.  $B - V$  ranges from  $+0.22 \pm 0.09$  to  $-0.25 \pm 0.14$ , and  $U - B$  ranges from  $-0.68 \pm 0.10$  to  $-1.04 \pm 0.10$ . The mean colors

TABLE 1  
JOURNAL OF OBSERVATIONS:  $UBV$  PHOTOMETRY

Run Number	Date (UT)	Telescope (m)	$V$	$B - V$	$U - B$	Notes <sup>a</sup>
2807.....	1983 May 3	0.9	14.91	-0.25	-0.95	1
2810.....	1983 May 4	0.9	14.40	-0.11	-0.93	1
2813.....	1983 May 5	0.9	15.21	-0.08	-0.73	1, 2
2813.....	1983 May 5	0.9	14.32	-0.05	-0.90	1, 3
.....	1984 Apr 3	0.8	14.96	-0.06	-0.90	4
.....	1984 Apr 4	0.8	13.63	-0.22	-0.99	4
2920.....	1984 Apr 8	0.9	14.07	-0.09	-0.97	1
2924.....	1984 Apr 9	0.9	14.51	-0.11	-0.91	1, 2
2926.....	1984 Apr 9	0.9	15.15	+0.01	-0.94	1, 3
2929.....	1984 May 1	2.1	14.96	-0.16	-1.01	1
2934.....	1984 May 2	2.1	16.95	-0.13	-1.03	1
2939.....	1984 May 3	2.1	16.91	+0.14	-0.92	1, 2
2945.....	1984 May 3	2.1	17.00	+0.03	-0.82	1, 3
2947.....	1984 May 4	2.1	15.26	-0.12	-1.03	1
2951.....	1984 May 5	2.1	16.96	+0.04	-0.98	1
2956.....	1984 May 6	2.1	17.11	+0.22	-1.04	1
2960.....	1984 May 7	2.1	16.21	-0.10	-0.68	1
2965.....	1984 Jun 1	0.9	14.32	-0.13	-0.85	1, 2
2967.....	1984 Jun 2	0.9	14.22	-0.05	-0.96	1, 3
2972.....	1984 Jun 5	0.9	14.61	-0.03	-0.89	1
3008.....	1985 Mar 19	0.9	13.77	-0.22	-1.01	5
3009.....	1985 Mar 20	0.9	13.92	-0.16	-0.95	5
3013.....	1985 Mar 22	0.9	14.24	-0.07	-0.96	5
3022.....	1985 Mar 23	0.9	16.00	-0.13	-0.92	5
3030.....	1985 Mar 25	0.9	14.47	-0.03	-0.93	5
3033.....	1985 Mar 26	0.9	15.3	...	...	6
3034.....	1985 Mar 27	0.9	14.4	...	...	6
3035.....	1985 Mar 28	0.9	14.4	...	...	6
3943.....	1985 Apr 19	0.9	15.33	-0.19	-0.93	5
3049.....	1985 Apr 22	0.9	13.99	-0.11	-0.97	5

<sup>a</sup> NOTES.—(1) Time-averaged differential photometry.  $\sigma \approx \pm 0.10$  mag. (2) Observation at beginning of night. (3) Observation at end of night. (4) All-sky photometry (H. G. Corwin, private communication).  $\sigma \approx \pm 0.05$  mag. (5) Instantaneous differential photometry.  $\sigma \approx \pm 0.13$  mag. (6) Estimated visual magnitude.  $\sigma \approx \pm 0.5$  mag.

of PG 1346+082 are consistent with those reported by Bern and Wramdemark (1973) for the variable DB white dwarf GD 358:  $B - V = -0.11 \pm 0.02$ , and  $U - B = -1.04 \pm 0.02$ . In addition, this mean  $U - B$ ,  $B - V$  agrees well with the theoretical colors predicted by Mayo *et al.* (1980) for a cosmic composition disk in outburst.

Figures 1 and 2 show the observed behavior of the colors  $B - V$  and  $U - B$  versus  $B$  magnitude, respectively. Figure 3 presents the two-color diagram of  $U - B$  versus  $B - V$ . The error bars are large, but there appears to be a correlation between color and magnitude: the system is redder at minimum light. Similar behavior is seen in variable-rate accretion systems—higher accretion rates usually imply higher temperatures and bluer colors.

### c) Harvard Meteor Program Data

A detailed accounting of the HMP is beyond the scope of this manuscript (see Whipple 1947); however, because few observers are familiar with this resource, we have included a few comments concerning the equipment and method of data acquisition in the Appendix.

Because the relatively slow, large-amplitude photometric variations have time scales on the order of a week and peak-to-peak amplitudes of 4 mag, we studied them using archival photographic data. The HMP data span 6 yr, and there were typically four exposures per hour, giving us coverage of PG

TABLE 2  
JOURNAL OF OBSERVATIONS: HIGH-SPEED PHOTOMETRY

Run Number <sup>a</sup>	Length (hr)	Telescope (m)	Date (UT)	HJED of Run Start (2,440,000. +)	Approximate B Magnitude <sup>b</sup>
r2786.....	3.36	2.7	1983 Apr 10	5,434.780481	...
r2791.....	3.11	2.7	1983 Apr 12	5,436.713648	...
r2793.....	8.08	0.9	1983 Apr 14	5,438.631161	...
r2801.....	1.67	0.9	1983 Apr 16	5,440.898597	14.10
r2806.....	1.98	0.9	1983 Apr 17	5,441.882955	...
r2900.....	5.71	0.9	1984 Apr 3	5,793.716043	15.08
r2908.....	6.48	0.9	1984 Apr 4	5,794.675420	13.63
r2919.....	5.64	0.9	1984 Apr 8	5,798.716088	14.16
r2930.....	6.22	2.1	1984 May 1	5,821.685047	15.12
r2937.....	2.81	2.1	1984 May 2	5,822.835013	17.08
r2940.....	3.39	2.1	1984 May 3	5,823.669362	16.87
r2949.....	4.48	2.1	1984 May 4	5,824.673959	15.38
r2952.....	5.42	2.1	1984 May 5	5,825.671493	16.92
r2999.....	2.22	2.1	1985 Jan 18	6,083.907718	...
r3003.....	1.39	2.1	1985 Jan 19	6,084.955179	...
s3490.....	1.71	0.9	1985 Mar 18	6,142.533659	...
s3491.....	4.31	0.9	1985 Mar 18	6,143.466568	...
s3492.....	4.76	0.9	1985 Mar 19	6,144.446814	...
s3494.....	4.60	0.9	1985 Mar 21	6,146.455105	...
r3014.....	4.72	0.9	1985 Mar 22	6,146.709164	14.24
s3495.....	1.53	0.9	1985 Mar 22	6,147.528637	...
r3021.....	4.61	0.9	1985 Mar 23	6,147.776098	15.66
s3496.....	1.62	0.9	1985 Mar 24	6,148.519179	...
r3031.....	3.58	0.9	1985 Mar 25	6,149.787274	14.47
s3497.....	2.53	0.9	1985 Mar 25	6,150.497480	...
r3042.....	6.54	0.9	1985 Apr 19	6,147.641346	...

<sup>a</sup> r denotes McDonald Observatory data. s denotes SAAO data.

<sup>b</sup> If available.

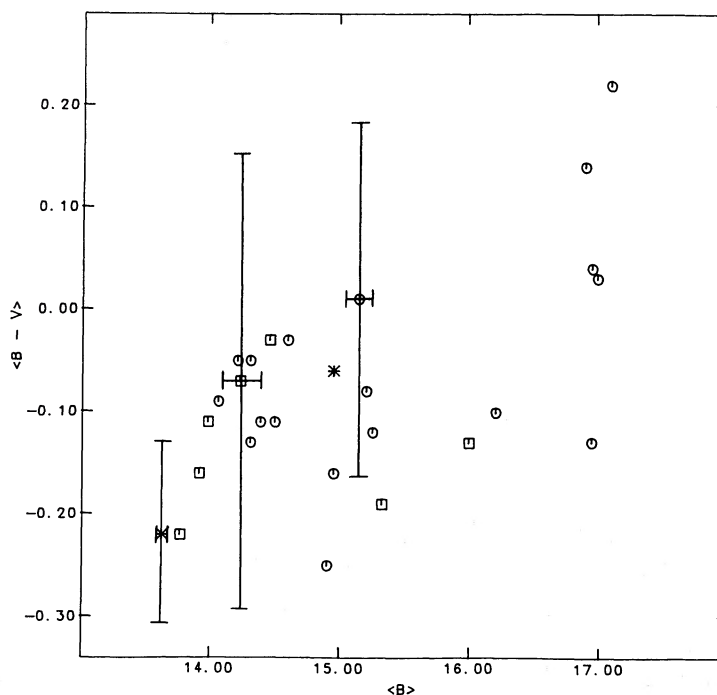


FIG. 1.—Color-magnitude plot for  $B-V$  vs.  $B$ . In the figure, the circles represent the time-averaged differential photometry observations, the squares the instantaneous photometric observations, and the asterisks the calibrated, all-sky photometric observations. Typical formal errors for the time-averaged differential observations are  $\Delta B = \pm 0.10$ ,  $\Delta(B-V) = \pm 0.14$ , and  $\Delta(U-B) = \pm 0.14$ ; for the instantaneous differential observations,  $\Delta B = \pm 0.13$ ,  $\Delta(B-V) = \pm 0.18$ , and  $\Delta(U-B) = \pm 0.18$ ; for the all-sky photometry observations,  $\Delta V = \pm 0.05$ ,  $\Delta(B-V) = \pm 0.07$ ,  $\Delta(U-B) = \pm 0.07$ . We have plotted one set of error bars for each of these three methods. The data suggest that in general the system is bluer in high state than in low state.

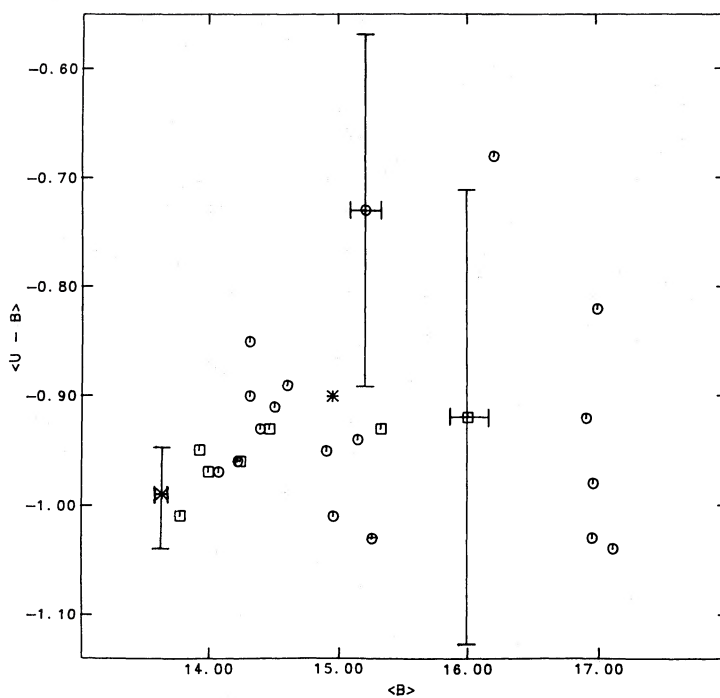


FIG. 2.—Color-magnitude plot for  $U-B$  vs.  $B$ . See Fig. 1 for a definition of the symbols and associated error bars. Here again, the system generally appears bluer at maximum light than at minimum light.

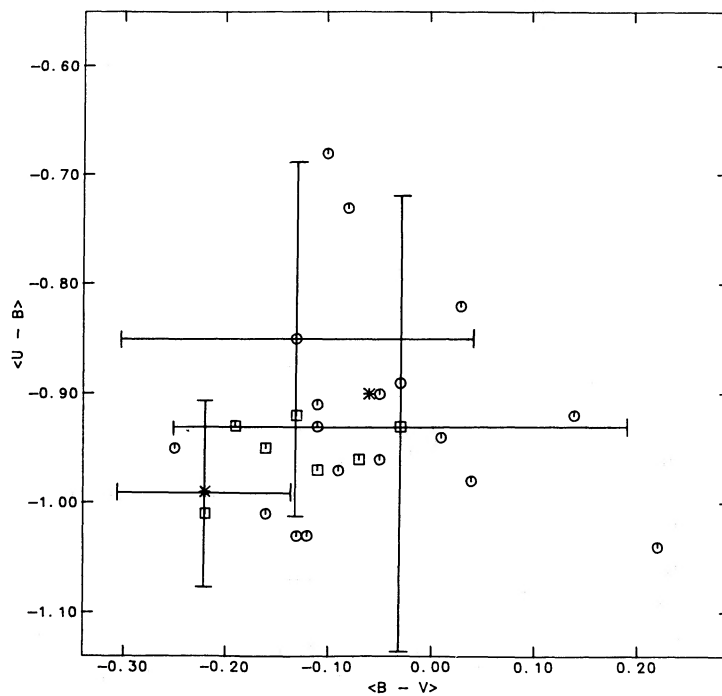


FIG. 3.—Color-magnitude plot for  $B-V$  vs.  $U-B$ . See Fig. 1 for a definition of the symbols and associated error bars.

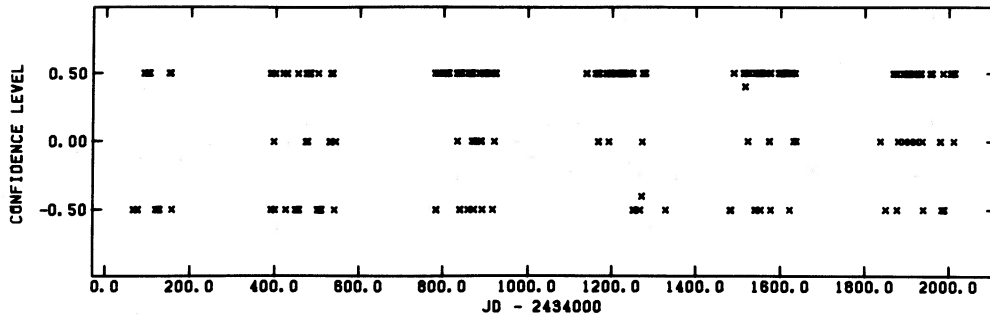


FIG. 4.—Light curve from the archival HMP photographic films. This figure presents the light curve obtained using the HMP data. The light curve spans 6 yr, from 1952 through 1957 (JD 2,434,066–2,435,016). If PG 1346+082 was brighter than the comparison star ( $V_{pg} \approx 14.0$ ), we assigned it a value of +0.5, if fainter a value of -0.5, and if the same brightness, a value of 0.0. Intermediate values were obtained when the films were averaged over the night.

1346+082 on roughly 1100 different films. Because of the variations in film quality, on each film we compared the brightness of the program object with that of a nearby field star which has  $m_{pg} \approx 14.0$ . After averaging all the data within a given night, we recorded the magnitude of PG 1346+082 as greater than (+0.5), less than (-0.5), or equal to (0.0) the brightness of the comparison star (i.e., equal to within approximately  $\pm 0.1$  mag. See Fig. 4).

We found that the system was as bright or brighter than the comparison star on roughly 74% of the films that were examined. We present the Fourier transform of the data and the associated spectral window in Figure 5. There is power present in the data that is not also present in the spectral window with a period of 4–5 days, suggesting the long-term variations are quasi-periodic. Moreover, because the minima are not strictly periodic with a single period, it is unlikely that they result from eclipses.

#### d) High-Speed Photometry: The Short Time Scale Variations

The details of our method of high-speed photometric data reduction are discussed by Kepler *et al.* (1982). The analysis of PG 1346+082 is complicated because the *character* of the light curve is variable. Figure 6 shows portions of four different light curves, which span the range of average  $V$  magnitude (*top to bottom*: 1984 April 4, April 8, May 4, and May 5); Figure 7 shows the four corresponding amplitude spectra (which are just the square root of the power spectra). The light curve at  $V = 13.6$  looks similar to the light curve of AM CVn (see Patterson *et al.* 1979); the light curve at  $V = 14.2$  shows similarity to the one above it, but with smaller amplitude; the light curve at  $V = 15.4$  is reminiscent of that of a non-radially pulsating white dwarf (cf. Robinson 1979); the light curve at  $V = 17.1$  shows flickering behavior similar to that found in the cataclysmic variable systems (cf. Shafter and Szkody 1984).

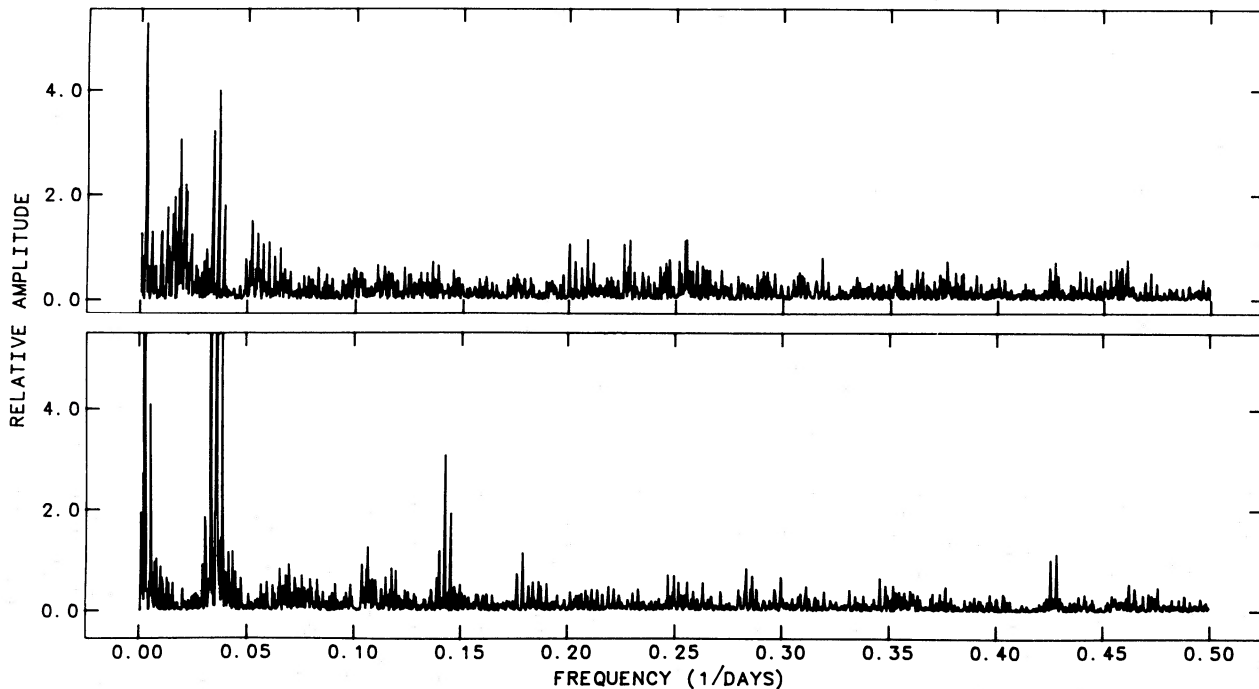


FIG. 5.—Fourier transform (amplitude spectra) of the data presented in Fig. 4 (*top panel*) and the spectral window taken about zero frequency (*bottom panel*). Peaks present in the transform of both the data and the spectral window are likely to be artifacts of the reduction process, and not correspondent to a real periodicity in the data. Note, however, that there is power present at roughly 4–5 days that is not present in the spectral window.

In the amplitude spectrum plot, two features in particular deserve mention. First, note that the 745 s peak is always present, even though the 1490 s period is lost in the noise in the  $V = 15.4$  spectrum—roughly 20% of our light curves do not show significant power ( $2\sigma$ ) above the noise at  $P = 1490$  s. Second, note the high-frequency band of power present in the  $V = 15.4$  spectrum, spanning the range 200–400 s. These periods are consistent with those we have found in solitary white dwarfs, where they arise from nonradial pulsations.

The persistent presence of the 745 s and 1490 s periodicities opened the possibility that they might be coherent from night to night and over the 4–5 day quasi period. The tool we used to help explore this possibility was a least-squares fit of a single sine curve to the data. Specifically, we fitted

$$I = A \sin \left[ \frac{2\pi}{P} (t - T_0) \right], \quad (1)$$

where the three free parameters of the fit were the period ( $P$ ), the semiamplitude ( $A$ ), and the time of axis crossing ( $T_0$ ). As an example, we will discuss our experiences with the 1984 April data.

First, we fitted to the individual runs. The period computed from the 1984 April 4 data was  $P = 1486 \pm 1.4$  s—more accurate than the 6 s accuracy needed to prevent cycle count ambiguity over 24 hr. Second, we combined the data sets from consecutive nights (1984 April 3–4) which gave us a period

accurate enough ( $P = 1487.3 \pm 0.3$  s) to phase to the 1984 April 8 data. The period obtained from these three data sets combined ( $P = 1490.03 \pm 0.07$  s) fell roughly  $10\sigma$  away from the previous period determination. We concluded that the periodicity is not strictly coherent.

We tried this exercise with the 745 s periodicity, and it did not maintain phase either. Furthermore, we have used several different pairs of adjacent nights from 1984 and 1985 as bases, and consistently find the maximum coherence time to be roughly 1 week—consistent with the time scale indicated by the periodogram of the HMP data, and with our qualitative impression of the time scale of large-amplitude variability. It is quite possible that the changes in the pulse shape affect the calculated  $T_0$  and hence prohibit our phasing together high-state and low-state light curves; unfortunately, our data are too sparse to allow us to bridge only among runs of any particular state—we could not avoid cycle count ambiguity in that case.

#### e) The Average Amplitude Spectrum

To increase the sensitivity for low-amplitude variations, we averaged together the power spectra of the nine longest light curves (and took the square root of the result to obtain the average amplitude spectrum; see Fig. 8). In order to average together spectra with lines of equal width, we truncated all the light curves to a uniform length corresponding to that of the shortest of these runs: 4.22 hr.

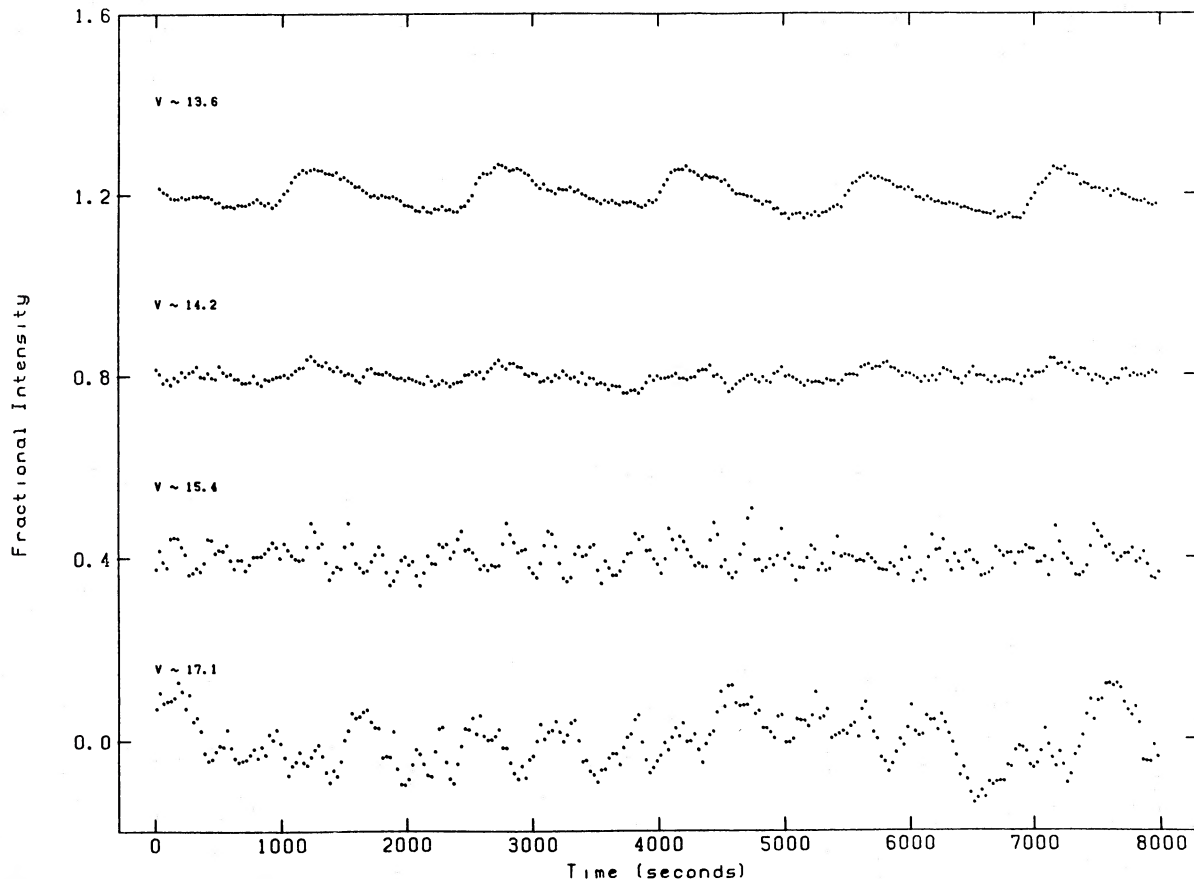


FIG. 6.—A summary of portions of the light curves of the system on the nights (top to bottom) 1984 April 4, April 8, May 4, and May 5 (UT), demonstrating the variable character of the light curves of PG 1346+082. The light curves have all been normalized about zero, and then constant values were added to the upper three to offset them.

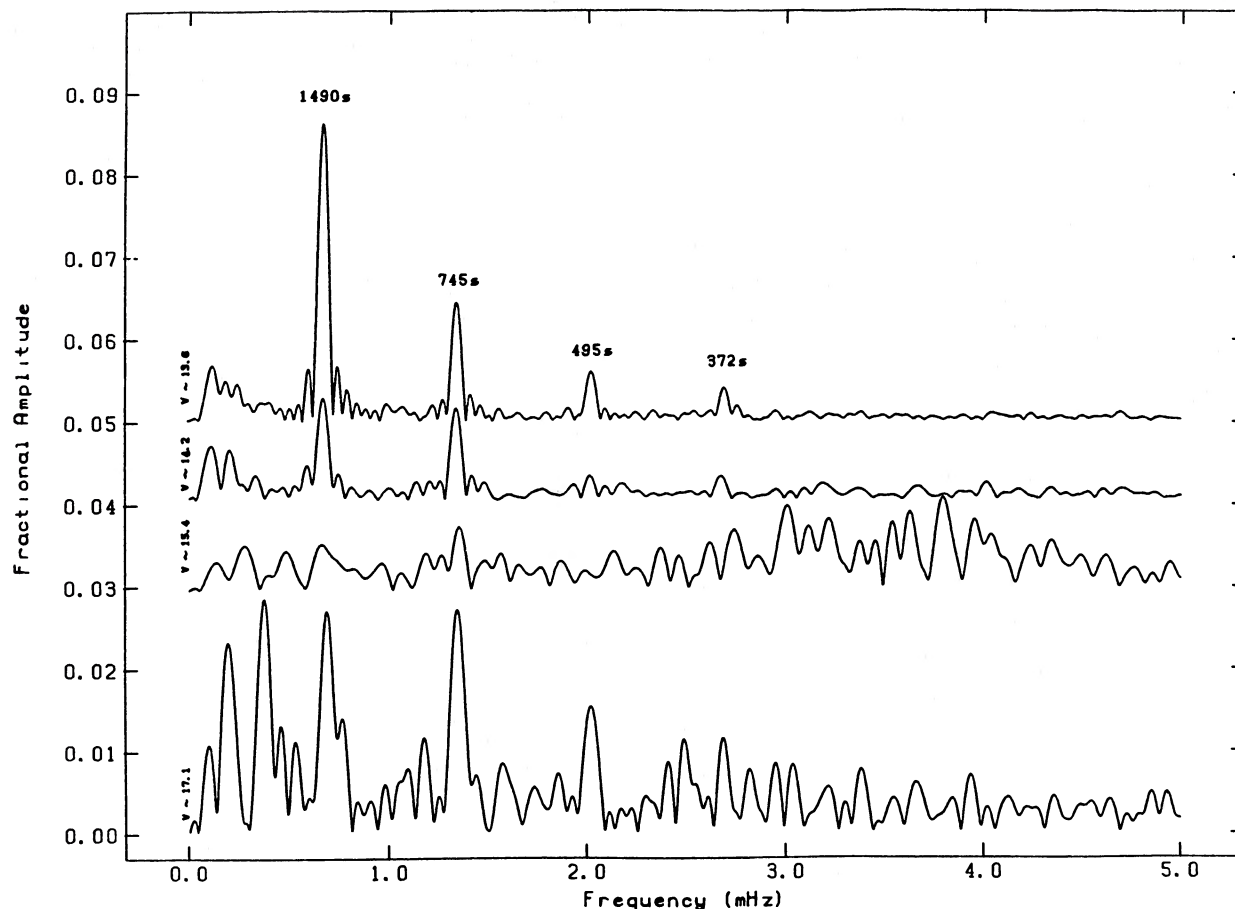


FIG. 7.—Amplitude spectra corresponding to the four light curves presented in Fig. 6. The low-frequency portions of the amplitude spectra corresponding to the light curves shown in Fig. 6. There is no significant power above the frequency 5 mHz, and so this portion of the amplitude spectra has not been shown. The four curves are plotted with the same vertical scale, but have been offset from each other by constant values.

We always look for simple relations among the periods found in spectra and in particular search for harmonic relations. The search proved fruitful in this case. We define 10,200 s and 1490 s as our two primary periods (for reasons given below), then we find that all of the other peaks found in the average spectrum are either harmonics of one of the two, or are linear combinations of the two. Although the 10,200 s peak is not so far above the noise that we can conclusively claim that it is real, it is suggestive in view of the peaks at its harmonics. Extended photometric coverage of this system should also remove any doubt concerning the reality of the 10,200 s period.

#### f) SAAO Data—Attacking the 10,200 Second Question

We scheduled simultaneous observing runs at McDonald Observatory and at the SAAO the week of 1985 March 18. During that week, useful high-speed photometric data were obtained at SAAO on four nights, and at McDonald on one night. We were fortunate on the night of 1985 March 22 (UT), because we both obtained long runs on the system. The time gap between our data sets is 90 minutes. Upon putting these two light curves (s3494 and r3014) on the same plot, it was evident to the eye that there was a long-period variation that connected the two. A nonlinear least squares, three-parameter fit of a single sine wave confirmed the periodicity evident to the

eye:

$$P = 9700 \pm 300 \text{ s}, \quad A = 6.7 \pm 1.4 \text{ mmag}, \\ T_0 = 363469 \pm 380 \text{ s}.$$

Next, we combined these data with the South African data from two nights previous (s3492). The nonlinear least-squares fit to these data was

$$P = 10197 \pm 42 \text{ s}, \quad A = 6.7 \pm 1.3 \text{ mmag}, \\ T_0 = 363852 \pm 460 \text{ s},$$

and finally, including run s3491, the fit was

$$P = 10201 \pm 30 \text{ s}, \quad A = 6.6 \pm 1.3 \text{ mmag}, \\ T_0 = 363865 \pm 540 \text{ s}.$$

Figure 9 shows the resulting fit together with the original data.

We tried to extend the fit off both ends, but were unsuccessful. On the earlier side, we have run s3490, which is too short to provide useful information for a 2.8 hr periodicity; on the later side, we have run r3021—a run in which sky counts (per second) received by the photometer exceeded star counts. Note that for these three fits, the formal errors in  $T_0$  get progressively worse as more data are added, even though the formal errors in the period and amplitude decrease as expected.

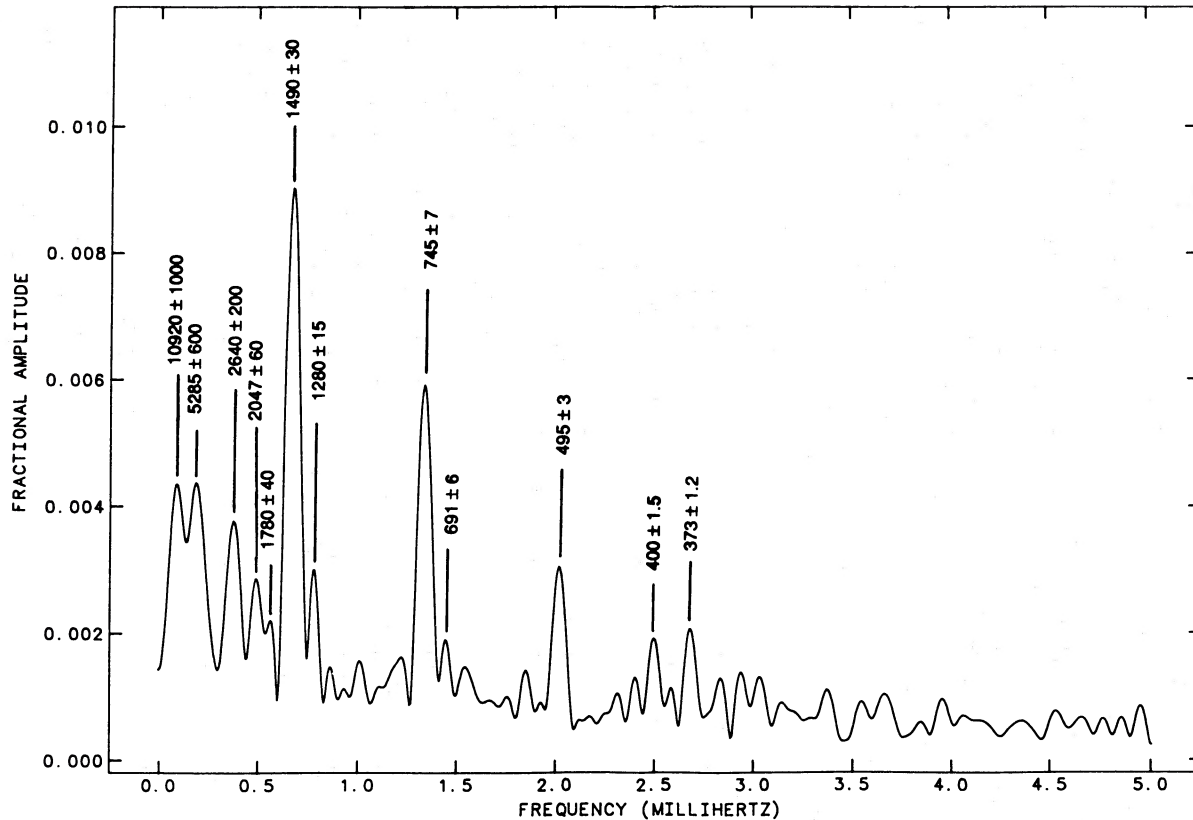


FIG. 8.—Average amplitude spectrum. This figure presents the square root of the average of the power spectra of the nine longest light curves. Before obtaining the individual power spectra, all of the light curves were truncated to 4.2 hr. The quoted errors correspond to  $\text{HWHM}/(9)^{1/2}$ .

This may suggest that the periodicity is not in fact coherent, in spite of its appearance to the eye; however, keeping in mind the problems encountered in attempting to phase the data with the 1490 s periodicity, we were not too surprised that this periodicity was not well behaved. Because these data (apparently) phase over only a few days, because the amplitude of the detected variability is so low, and because our method of data acquisition is not optimized for detecting long periods, we still cannot be completely certain this periodicity is real. The data are clearly suggestive, and for now we must be content with that.

### III. SPECTROSCOPY

#### a) The Observations

Our spectroscopic observations were obtained using an intensified image dissector scanner (IDS) (Rybski, Mitchell, and Montemayor 1977) at the Cassegrain focus of the McDonald observatory 2.7 m reflector, an intensified photon-counting

Reticon spectrograph on the Multiple Mirror Telescope (MMT; Latham 1979), and an electronic CCD spectrograph (Tull, Vogt, and Kelton 1979) at the Cassegrain focus of the McDonald Observatory 2.1 m. In addition, we have spectroscopic data obtained with the *International Ultraviolet Explorer Satellite (IUE)*.

The McDonald IDS observations were obtained by A. Cochran and E. S. Barker on the night of 1984 March 31 (UT), and by B. Wills on the night of 1984 May 31 (UT) (see Fig. 10 for the average of these spectra). The dispersion used was  $116 \text{ \AA mm}^{-1}$ , the resolution was  $11.6 \text{ \AA}$ , and the spectral coverage was 3800 to 6500  $\text{\AA}$ . Each individual integration was 50 s long. The total integration length on 1984 March 31 was 54 minutes, and on 1984 May 31, 20 minutes.

The MMT data were obtained by J. L. on the nights of 1983 July 5 (UT) (Fig. 11) and 1985 March 31 (UT) (Fig. 12). The dispersion used was  $12.9 \text{ \AA mm}^{-1}$ , the resolution was  $1 \text{ \AA}$ , and the spectral coverage was 4080 to 5040  $\text{\AA}$ . For the first night's

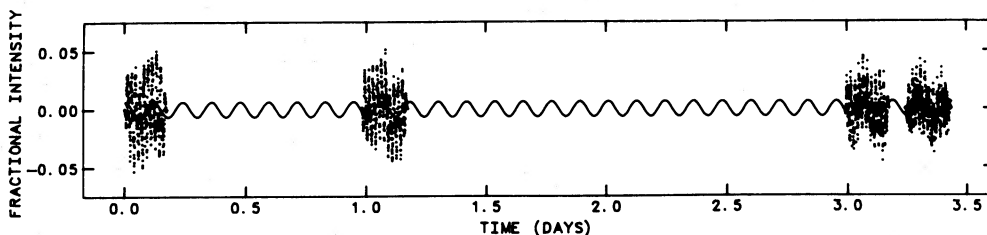


FIG. 9.—The 10,200 s period fit plotted over the data. The data were binned into 5 minute intervals. What appears to be a “noise band” is the envelope of the 1490 s variations.

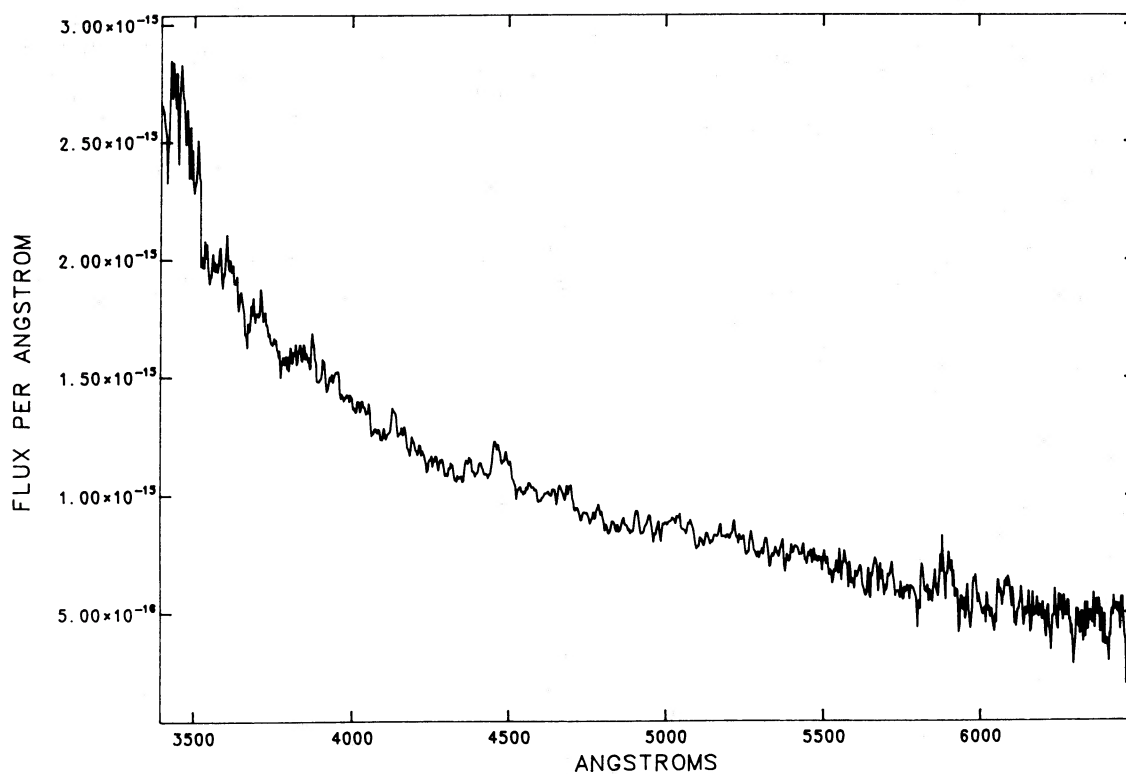


FIG. 10.—1984 IDS low-state spectrum. The modest signal-to-noise ratio of this spectrum obscures nearly all features; however, we find a weak emission feature at He I 4471 Å, and possibly one at 5876 Å. The former feature was present in both channels of the spectrograph in both input spectra. The latter was not present in both input spectra.

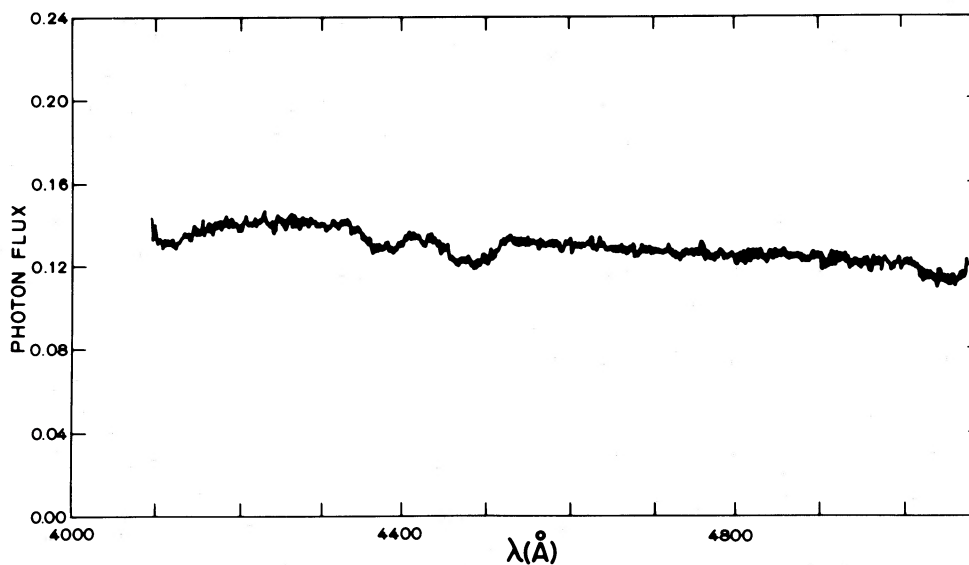


FIG. 11.—1983 MMT high-state spectrum. The line profiles of this spectrum closely resemble those of AM CVn (see Fig. 14); both objects show asymmetric line profiles that are shallower than single DB white dwarfs, both lack the usually strong He I 4713 Å line in their spectra, and both show He I 4388 Å comparable in strength to He I 4471 Å.

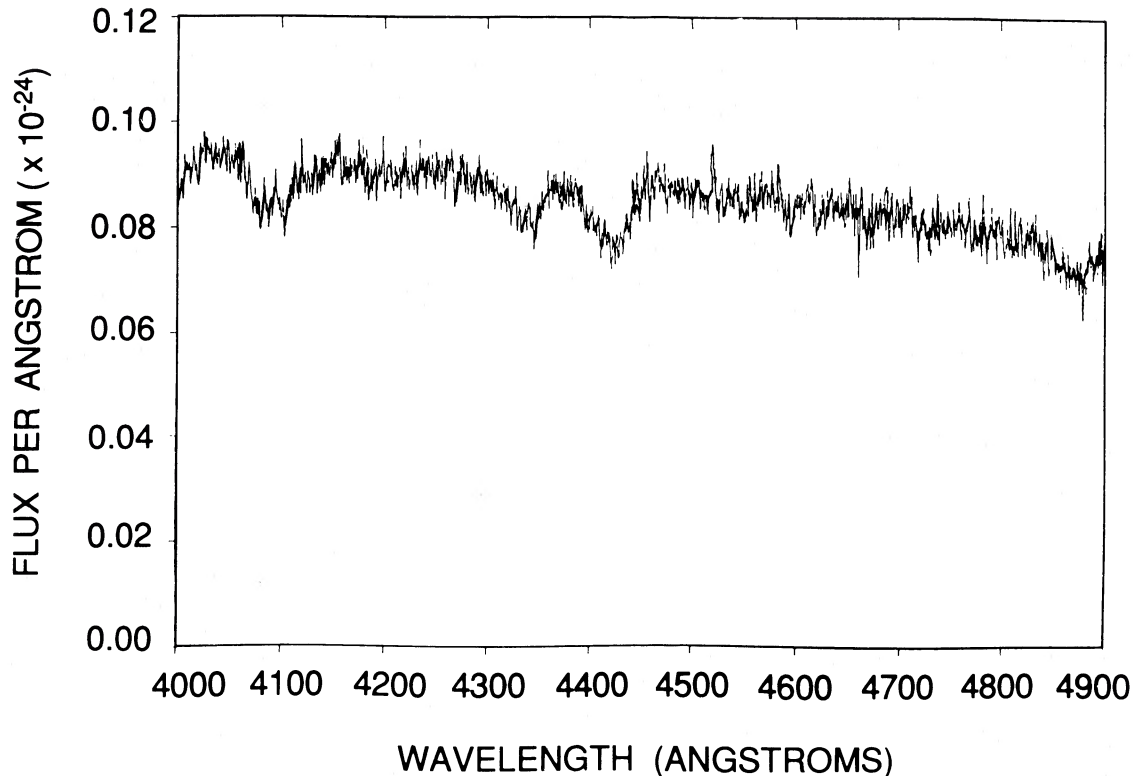


FIG. 12.—1985 MMT spectrum. This figure demonstrates that the asymmetry found in the line profiles can change sense.

data, the integrations were 115 s long; the latter used integrations of 10 minutes each. The total integration on 1983 July 5 was 32 minutes, and on 1985 March 31, 20 minutes.

Our time-resolved observations were obtained at McDonald Observatory by F. V. H. on the nights 1984 April 4, 6, 8, and 9 (UT) using the CCD spectrograph attached to the 2.1 m telescope. The dispersion used was  $60 \text{ \AA mm}^{-1}$ , the resolution was  $6 \text{ \AA}$ , and the useful spectral coverage was 3950 to 4780  $\text{\AA}$ . On the first night (when the system was near maximum) the integration times were 2.5 minutes, and on the following nights (when the system had faded somewhat) the integration times were typically 5 minutes.

A spectroscopic scan of PG 1346 + 082 was secured by G. W. on 1984 January 9 using the intensified image dissector scanner (IIDS) attached to the 2.1 m telescope at Kitt Peak. The instrumental configuration and data reduction are detailed in Wegner (1983). The coverage was from 3300 to 6700  $\text{\AA}$ , with a resolution of  $17 \text{ \AA}$ .

Finally, *IUE* data were obtained from G. W. on 1983 March 24 and by J. L. and F. W. on 1984 May 17. Specifics for these exposures, which included both long-wavelength and multiple short-wavelength frames at low ( $7 \text{ \AA}$ ) resolution, are summarized in Table 3.

#### b) Overview of the Results

All the spectra show only lines of neutral helium, and the line profiles are broad ( $\sim 100 \text{ \AA}$ ) and shallow ( $\sim 10\%$ )—indicating an evolved object in two ways. First, the broad spectral features are a sign of either pressure broadening in the atmosphere of a degenerate object, or a combination of Doppler broadening ( $\pm 2500 \text{ km s}^{-1}$ ) and pressure broadening in an accretion disk surrounding a compact mass accretor. Second, the chemical purity of the helium photosphere implies

earlier gravitational settling of heavier elements in an evolved star—again indicating high gravities.

The high-state spectrum of PG 1346 + 082 is similar to that of AM CVn (see Fig. 13, adapted from Robinson and Faulkner 1975). Both objects have line profiles that are considerably shallower than single DB white dwarfs (cf. Liebert 1977), both display asymmetric line profiles, and both are missing the usually strong He I 4713  $\text{\AA}$  in their spectra (Greenstein 1958) but have rather strong He I 4388  $\text{\AA}$ . We note here that because the line profiles are quite dissimilar to those observed in single DB white dwarfs, no attempt was made to fit theoretical line profiles or to determine equivalent widths. Also, to the authors' knowledge, theoretical line profiles of disks of pure helium have not been published; however, theoretical studies of cosmic abundance disks do not show the asymmetry observed here (cf. Mayo *et al.* 1980).

Compare Figures 11 and 12: We see that the asymmetry of the line profiles of PG 1346 + 082 can change sense. Robinson and Falkner (1975) proposed that the peculiar line profiles in AM CVn could be modeled crudely by adding an optically thin

TABLE 3  
JOURNAL OF OBSERVATIONS: *IUE*

Image Number	$t_{\text{exp}}$ (minutes)	$V$
SWP 19534 .....	20	$\sim 14.2$
SWP 19535 .....	20	$\sim 14.2$
SWP 19536 .....	15	$\sim 14.2$
LWR 15571 .....	40	$\sim 14.2$
SWP 23034 .....	60	...
SWP 23035 .....	60	...
LWP 3377 .....	60	...

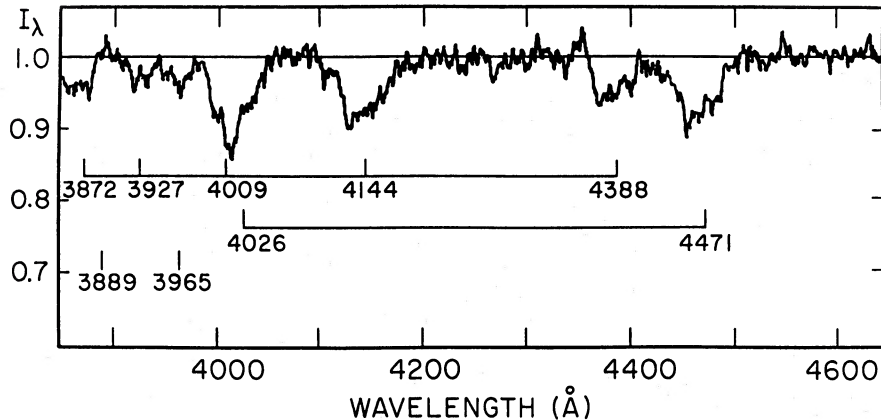


FIG. 13.—The spectrum of AM CVn, presented for comparison with PG 1346+082 (adapted from Robinson and Faulkner 1975)

helium capture-cascade emission-line spectrum (Brocklehurst 1972) to a normal DB white dwarf absorption spectrum. If this is the case, and if the same mechanism is working in PG 1346+082, then a natural explanation for the observed variable asymmetry may be the time-dependent viewing angle of the system's accretion hot spot—a hypothesis that should be testable using time-resolved spectroscopy on a large telescope.

Figure 10 shows the average of the low-state spectra. There are no strong features evident above the noise, but we find a weak emission feature at 4471 Å. Thus, the spectral behavior of PG 1346+082 is reminiscent of that observed from the dwarf novae (absorption features when in high state, and emission features when in low state), but it is far less dramatic here. We need to obtain a high signal-to-noise ratio, low-state spectrum of this object to study the emission feature at 4471 Å; unfortunately, because the object is at minimum light so rarely, this observation will be difficult to obtain.

#### c) Time-resolved Spectroscopy

Because we wished to resolve a 25 minute spectroscopic period (if present), our exposures were relatively short. Unfortunately, because our detector was not photon-count-limited, but was instead electron readout-noise-limited at fainter magnitudes, the signal-to-noise ratios of the individual spectra are particularly poor.

We have examined spectra of PG 1346+082 for both secular variations within a night, and variations over the 25 minute and 2.8 hr photometric periodicities. To determine if the spectra underwent secular variations throughout the night, we averaged spectra over a 1 hr interval and moved the center of this window in steps of one-half hr. We detected no significant variations at our signal-to-noise ratios. When co-added into phase intervals covering 0.25 of the 25 minute photometric periodicity, the data again revealed no significant variations. Similarly, we found nothing when the spectra were co-added into phase intervals covering 0.25 of the 2.8 hr photometric periodicity.

The MMT data of 1983 July 5 were recorded in 120 s scans (spanning a total of 32 minutes). Examination of subsets of a 25 minute period did not reveal conclusive evidence for spectroscopic variations because of a marginally insufficient signal-to-noise ratio; however, it is possible that the co-addition of a few cycles of data of this quality could yield a detection of radial velocity variations.

#### d) The Ultraviolet Spectrum and Overall Energy Distribution

Figure 14 presents the ultraviolet energy distributions from the two *IUE* observations; in each case, the separate SWP exposures on each of the two runs have been co-added, and fluxes plotted for both cameras are binned over approximately 60 Å intervals. The *V* magnitude estimated from the *IUE* fine error sensor (FES) for the 1983 data is also plotted. For the 1984 observations, no such information is available as the fainter target was acquired by blind offset; however, we do have available data from the 1984 January 9 Kitt Peak IIDS spectrum covering 3300–6700 Å. The entrance aperture was 6", and so the data are spectrophotometric; we show the binned data points. PG 1346+082 was almost 2 mag brighter at ultraviolet wavelengths during the 1983 observations; the estimated  $V = 14.2$  indicates that it was near maximum brightness then. Crude fitting of theoretical high-gravity, pure-helium models to the 1983 data yields a temperature of roughly 22,000 K or 25,000 K, and to the 1984 data, roughly 17,000 K or 18,000 K, using the models of Koester (1980) and Wesemael (1981), respectively (cf. Liebert *et al.* 1986). These fits are shown plotted over the data. Modeling the ultraviolet energy distribution with a single-temperature photospheric model may be inappropriate, because the inferred accretion disk probably contributes substantially at these wavelengths. However, the quoted temperatures should be characteristic of those present in such a disk.

## IV. DISCUSSION

### a) The Model

Any model of this system must satisfy the following constraints:

1. The presence of large-amplitude (4 mag) photometric variability that exhibits a 4–5 day quasi period.
2. The presence of large-amplitude ( $\sim 10\%$ ) photometric flickering in the low-state light curves.
3. A spectrum that varies from showing only broad ( $\sim 100$  Å) shallow ( $\sim 10\%$ ) He I absorption lines, to showing only weak He I emission features (i.e., no He II, and no other elements, including hydrogen, are observed in any of our spectra).
4. A characteristic temperature of  $\sim 20,000$  K, and the fact that the system is not a strong X-ray source.

The above constraints are sufficient to narrow the number of

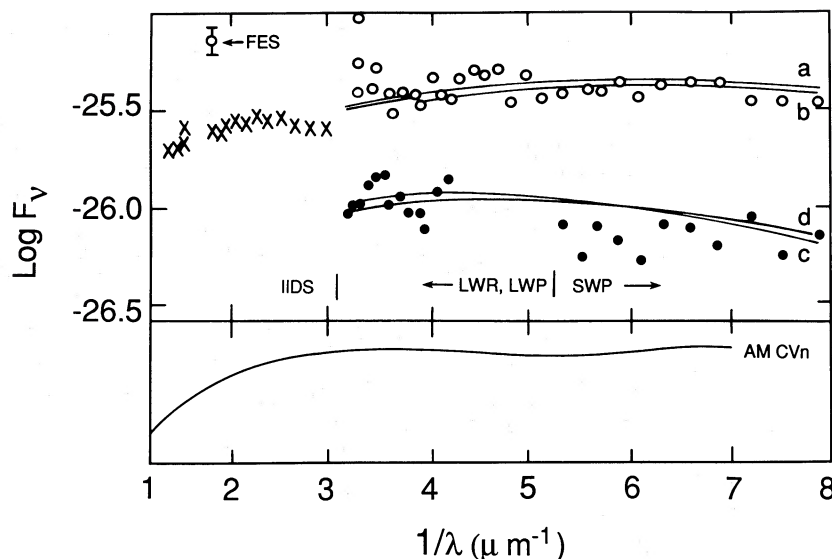


FIG. 14.—*IUE* flux distribution. The top panel shows the combined optical and ultraviolet flux distributions. The open circles represent the 1983 data, and the solid circles represent the 1984 data. The crosses correspond to the 1984 January 9 Kitt Peak IIDS intermediate-state spectrum. The 1984 data in the 2000–2500 Å range, obtained with the less-sensitive LWP camera, have been removed. Also shown are fits to the continuum. Fits *a* and *c* correspond, respectively, to the 22,000 K and 18,000 K models of Koester (1980), and fits *b* and *d* correspond, respectively, to the 25,000 K and 18,000 K models of Wesemael (1981). Note that fits *a* and *b* have been offset from each other slightly to avoid confusion. The bottom panel shows the flux from AM CVn, from Greenstein and Oke (1982), for comparison.

plausible models to one; below, we outline this process in some detail.

The rapid photometric flickering observed in PG 1346+082 is the classic indicator of mass transfer in a close binary system. Large-amplitude, quasi-periodic variability is the identifying feature of the dwarf novae, a subclass of the cataclysmic variables; the observed large-amplitude variability in PG 1346+082 is similar in many ways. The manner of spectroscopic variability (broad absorption lines at maximum, emission lines at minimum) also mimics that seen in the dwarf novae.

The spectral features we observe are  $\sim 100$  Å wide—a signature of either pressure broadening in the atmosphere of a single degenerate object, or of both pressure and Doppler broadening in an optically thick accretion disk surrounding a compact mass accretor.

We detect only features of He I in our spectra. The only objects observed in nature which show *pure* helium spectra are the DB white dwarfs. We therefore identify the mass-losing star in this system as degenerate helium star.

The characteristic temperature of PG 1346+082 is 15,000–25,000 K, and the system is not observed to be a strong X-ray source (J. Osborne and N. White, private communication). Thus, the accreting object in PG 1346+082 cannot be a neutron star or a black hole. The absence of detected He II in the visible places an upper limit on the temperature of the hottest gas visible and also rules out an accretor more compact than a white dwarf.

We therefore conclude that PG 1346+082 is an IBWD system. In addition to the arguments leading to this conclusion, we have other data that we can test for consistency against this model:

If the high-state spectrum has no significant contribution from emission processes, then the near-equal strengths of the high-state He I absorption lines 4388 and 4471 Å suggest origin in an environment where  $\log(g) \approx 6$  (cf. Hunger *et al.* 1981)—consistent with the expected gravity in an optically-thick disk.

If the system is an interacting twin degenerate, then the orbital separation must be small (so that the compact secondary may fill its Roche lobe), and hence the orbital period must be short. Because the 1490 s periodicity is nearly always found, it is possible that it is in fact the orbital period, although we have not been able to demonstrate this.

We have observed photometric variations in the 200–400 s range and mentioned that these are consistent with the periods observed in the pulsating white dwarf stars. We note that the derived *IUE* high-state temperature, 25,000 K, is consistent with membership in the instability regime for helium atmospheres (cf. Liebert *et al.* 1986). The lack of long-term coherence in these variations could be an indication that some, at least, arise in the helium accretion disk.

In the following sections, we explore the interacting twin-degenerate model for theoretical consistency with our data and discuss some of the implications of the model.

#### b) Mass-Transfer Rate

The maximum *B* band flux from the system is roughly a factor of 50 greater than the minimum flux. To calculate the mass transfer rate at maximum light we assume first that the luminosity at *minimum* light is dominated by the white dwarfs themselves ( $L_{\min} \approx 0.01 L_{\odot}$ ) and that the mass transfer rate is negligible ( $\dot{M}_{\min} \approx 0$ ), and second that the luminosity at maximum light is dominated by a disk and boundary layer with luminosity  $L_{\text{acc}} \approx 50L_{\min}$ . We then use the relation from Lynden-Bell (1969) for the accretion luminosity  $L_{\text{acc}}$ :

$$L_{\text{acc}} = \alpha \frac{3GM\dot{M}}{r_I} \left[ 1 - \frac{2}{3} \beta \left( \frac{r}{r_I} \right)^{1/2} \right], \quad (2)$$

where  $\alpha$  and  $\beta$  are dimensionless constants of order unity, and  $r_I$  is the inner radius of the accretion disk, taken to be  $5 \times 10^8$  cm. We find  $\dot{M}_{\max} \approx 2 \times 10^{-10} M_{\odot} \text{ yr}^{-1}$ , consistent with mass transfer rates of the mixed-composition cataclysmic variables. Because of uncertainties in the role of the residual disk, and in

the intrinsic luminosities of the stellar components, this result is probably reliable only to an order of magnitude; however, we note that our derived rate of mass transfer is consistent with the instability regime for helium disks as discussed by Smak (1983) and Cannizzo (1984). Furthermore, Smak notes that the derived mass transfer rate of AM CVn is too high to be in the instability regime (implying a thick disk, consistent with the observed absorption features), and that the rate in GP Com is too low to be in the instability regime (implying a thin disk, consistent with the observed emission features).

### c) System Geometry

A schematic of our model is shown in Figure 15 (the figure is roughly to scale for  $M_2/M_1 = 0.03$ ). Using some simple, reasonable assumptions we can investigate the properties of the secondary star; specifically, we assume that the system contains only two stars, that the secondary star fills its Roche lobe, and that the primary has mass  $M_1 \approx 1 M_\odot$ .

Let  $\mu$  represent the mass fraction  $M_2/(M_1 + M_2)$ . It follows (Faulkner, Flannery, and Warner 1972) that the mean radius of the Roche lobe  $R_L$  is related to the orbital separation  $a$  by:

$$R_L/a = 0.459\mu^{1/3} \quad (3)$$

(the intrinsic errors in this expression not exceeding  $\sim 3\%$  for

$\mu < 0.5$ ). Next, combining this expression with Kepler's law, we obtain an expression for the mean density of the secondary which is independent of the total mass of the system:

$$\begin{aligned} \langle \rho \rangle &= \frac{3M_2}{4\pi R_L^3} = \frac{3\pi}{(0.459)^3} \frac{1}{GP^2} \\ &= \frac{1.47 \times 10^9}{P^2} \text{ g cm}^{-3}, \end{aligned} \quad (4)$$

where the period is in seconds. This relation between  $P$ ,  $M_2$ , and  $R_L$  is shown in Figure 16, along with several mass-radius relations of interest. We can get rough estimates of the mass and radius of a Roche lobe-filling secondary by finding the intersection of the EOS of interest with the period. We emphasize that these are rough estimates only, and note that it is conceivable that tidal interaction of the primary induces formation of an atmosphere of the secondary, giving the secondary an effective radius twice or more that of an isolated white dwarf star of equal mass. In this case, the Roche lobe will "touch" the star at this greater radius, and both the mass and average density of the star itself could be substantially greater than the result of equation (3) would indicate. There are two candidate photometric periodicities we will investigate: 1490 and 10,200 s.

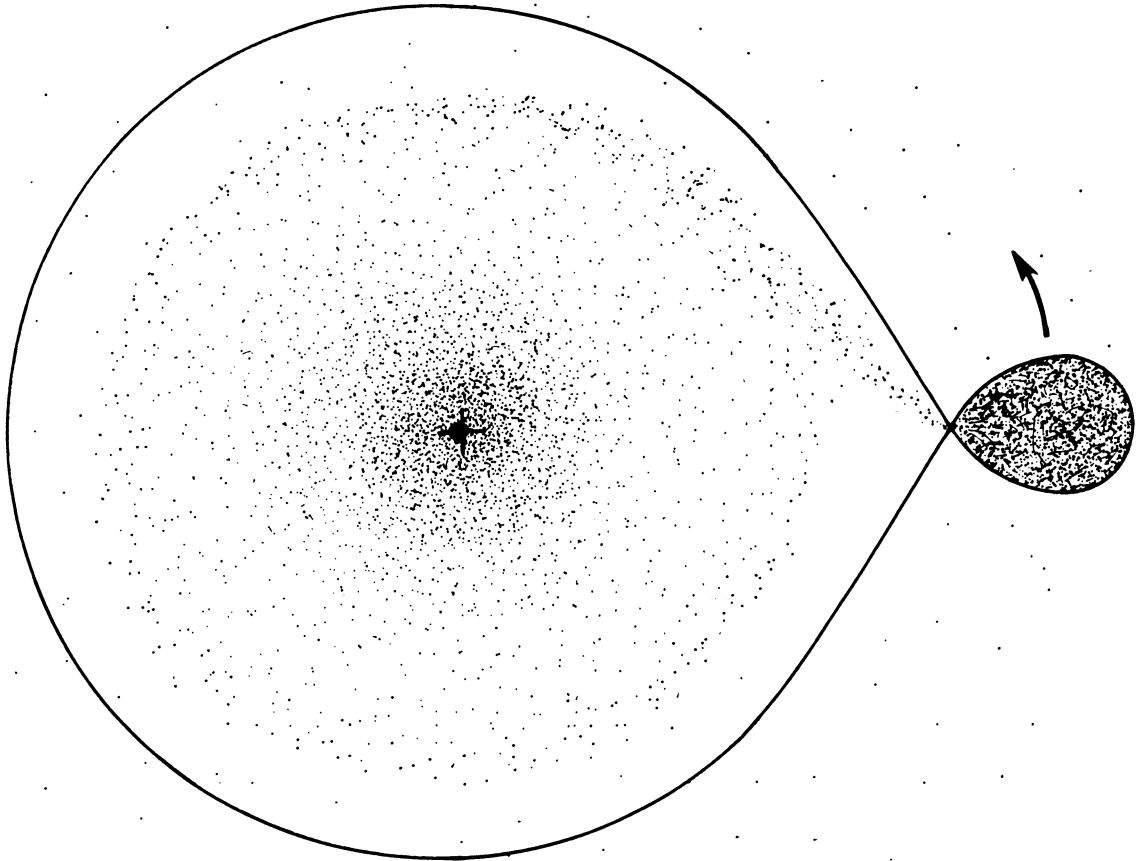


FIG. 15.—A schematic representation of the PG 1346+082 system. This diagram was generated using a mass ratio ( $M_1/M_2$ ) of 0.02 and tables from Kopal (1978; for reference, the two stars are roughly  $0.3 R_\odot$  apart). The barycenter is marked with a plus; note that it lies *within* the primary. Because the matter passing through the inner Lagrangian point already has circular orbital angular momentum, the accretion disk fills the Roche lobe about the primary.

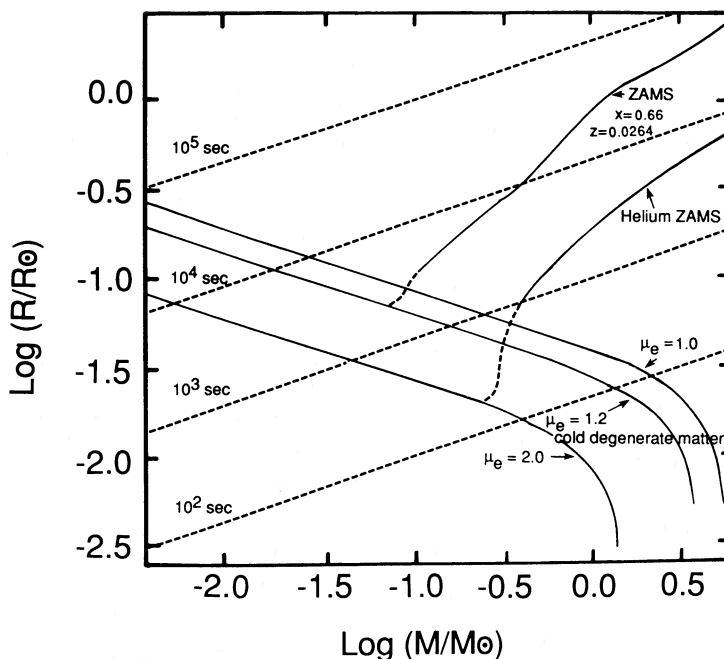


FIG. 16.—Lines of constant period (dashed lines) in a plot of secondary radius ( $\log R_2$ ) versus its mass ( $\log M_2$ ) for lobe-filling secondaries along with various equations of state (solid curves). A rough estimate of the mass and radius of a Roche lobe-filling secondary can be found by finding the intersection of the EOS of interest with the period of interest (adapted from Faulkner, Flannery, and Warner 1972).

i)  $P_{\text{orb}} = 1490 \text{ s}$

Using relation (3) above, we find  $\langle \rho \rangle = 645 \text{ g cm}^{-3}$ . In Figure 16, the line for  $P = 1490 \text{ s}$  intersects the helium EOS line twice, in the He-ZAMS regime ( $M_2 \approx 0.56 M_\odot$ ), and also in the degenerate EOS regime  $M_2 \approx 0.03 M_\odot$ . We ruled out the He-ZAMS star above. Therefore, assuming  $P_{\text{orb}} = 1490 \text{ s}$  implies that  $M_2 \approx 0.03 M_\odot$ , and from this it follows that  $a \approx 0.3 R_\odot$ .

ii)  $P_{\text{orb}} = 10,200 \text{ s}$

Assuming  $P_{\text{orb}} = 10,200 \text{ s}$  in equation (3) above, we find  $\langle \rho \rangle = 14 \text{ g cm}^{-3}$ . In this case, the only plausible candidate for the secondary star a very low mass DB white dwarf star. The determined mass,  $M_2 \approx 0.005 M_\odot$ , is uncomfortably low—roughly 5 times the mass of the planet Jupiter—suggesting that the 10,200 s periodicity, if it is not an artifact, is not the binary period.

In conclusion, we tentatively identify the 1490 s periodicity with the orbital period of the system and suggest that the mass of the secondary is of order  $0.02 M_\odot$ . As discussed in § II, the 1490 s periodicity does not maintain phase, and this argues against it being the orbital period; however, it is possible that the 1490 s periodicity is intrinsically coherent but appears not to be because of the changing disk size and luminosity—similar to the SU UMa stars (Vogt 1980).

## V. SUMMARY AND CONCLUSIONS

The data allow us to propose an unambiguous model for PG 1346+082: an interacting binary white dwarf model, similar to the models proposed for AM CVn and G61-29. In this context, we find some exciting prospects:

1. The “outbursts” of the system may be similar in physical origin to the dwarf novae outbursts. Because the thermodynamics of a pure-helium accretion disk should be easier to model accurately than those of a solar composition system, PG

1346+082 may help solve the puzzle of dwarf novae outbursts.

2. If indeed the temperature of the system varies within the DB instability strip, then we may be afforded the opportunity to map the boundaries of this strip.

3. Because we believe we are observing material transferred from the compositionally stratified remnant of a main-sequence star, we are seeing material brought to light in the accretion flow which has been processed in the stellar core of the secondary (cf. Nather, Robinson, and Stover 1981).

The identification of PG 1346+082 as an interacting twin degenerate star increases the likelihood that a similar model is appropriate for AM CVn as well, even though its orbital period has not yet been identified. The optical spectra of AM CVn and of PG 1346+082 outside of minimum are virtually identical. We have shown that the only plausible origin for the PG 1346+082 spectrum is in an optically thick accretion disk. We cannot rule out the (faint) possibility that nature is capable of making such a unique spectrum in two different ways; however, we consider it far more likely that AM CVn exhibits a helium disk in a state of “permanent outburst,” analogous to the UX UMa class of nova-like variables.

Clearly, PG 1346+082 is an object which merits further study. It would be useful to obtain time-resolved spectroscopic observations using a more sensitive instrument and/or a larger telescope than we had available for this investigation. We would also benefit from extended high-speed photometric coverage, preferably from three or more sites around the globe. In addition to helping with the 2.8 hr periodicity, such observations could catch the star undergoing a transition from one photometric character to another and might allow us to derive an empirical model for the pulse shape as a function of magnitude. We also hope that the observations we have presented will stimulate further theoretical investigations of the dynamics of the accretion process which include the simplifying (and physical) assumption of a pure-helium gas.

We are grateful to E. L. Robinson and J. A. Hill for useful discussions. In addition we thank E. L. Robinson, S. Balachandran, J. A. Hill, H. G. Corwin, and B. P. Hine III, for providing photometric data; E. Barker, A. Cochran, and B. Wills for providing individual optical spectra; J. Osborne and N. White for communicating their *EXOSAT* results; and H. J. Smith for suggesting and supporting our investigation of the archival Harvard Meteor Program films. We thank the personnel of the Harvard Plate Stacks for their assistance. Also, we are grateful to the referee who provided a number of helpful suggestions;

these forced us to reconsider the strength of our model, and reconstruct our argument. This work was supported in part by the National Science Foundation under grants AST 82-18624 through Steward Observatory, AST 81-08691 and AST 83-16496 through the University of Texas and McDonald Observatory, AST 83-19475 through Dartmouth College, in part by NASA (*IUE*) grant 5-38 and NAG 5-287, in part by the Foundation for Research Development of the CSIR of South Africa, and in part by the Natural Sciences and Engineering Research Council of Canada.

## APPENDIX

### HARVARD METEOR PROGRAM DATA BACKGROUND

The program was in full operation from 1952 to 1957, and the goal of the observing program was to determine the trajectories, velocities, and decelerations of meteors in Earth's upper atmosphere. These data could then be used in conjunction with theoretical models to determine atmospheric densities at heights of 50–120 km. The Program personnel used two Super-Schmidt cameras with rotating shutters placed  $\sim 30$  km apart, both watching the same volume of space in Earth's atmosphere, thus giving a stereoscopic image. They took data on every clear (not necessarily photometric) moonless night, exposing films at the rate of four per hour. The limiting magnitude of these films is  $V_{pg} \approx 14.5$ .

Because the focal surface of the cameras is a convex sphere of radius equal to the focal length (20 cm) photographic film pressed into the shape of a section of sphere had to be used. To

cover the  $\sim 52^\circ$  field of view of the Super-Schmidt cameras, the chordal diameter of the films needed to be 17 cm. The plate scale of the films is quite large ( $\sim 2.6 \text{ cm}^{-1}$ ); and the images quite small, spread over only a few grains of emulsion. Because of this, grain defects and variations provided a sizable source of error. This problem was compounded because a photographic emulsion suffers appreciably more distortion when placed on film rather than on glass; furthermore, the process of heating and pressing degraded some film's response.

For the reasons listed above, the stellar images seemed to "float around," sometimes making it difficult to determine if the image of the object was real but its position misrepresented, or if the "image" was the result of a film imperfection. In summary, the quality from film to film—and even between two different spots on the same film—was quite unpredictable.

## REFERENCES

- Bern, K., and Wramdemark, S. 1973, *Lowell Obs. Bull.*, No. 161.  
 Brocklehurst, M. 1972, *M.N.R.A.S.*, **157**, 211.  
 Cannizzo, J. K. 1984, *Nature*, **311**, 443.  
 Faulkner, J., Flannery, B., and Warner, B. 1972, *Ap. J. (Letters)*, **175**, L79.  
 Green, R. F., Schmidt, M., and Liebert J. 1986, *Ap. J. Suppl.*, **61**, 305 (PG).  
 Greenstein, J. L. 1958, *Handbuch der Physik*, **50**, 161.  
 Greenstein, J. L., and Oke, J. B. 1982, *Ap. J.*, **258**, 209.  
 Hunger, K., Gruschinske, J., Kudritzki, R., and Simon, K. P. 1981, *Astr. Ap.*, **95**, 244.  
 Kepler, S. O., Robinson, E. L., Nather, R. E., and McGraw, J. T. 1982, *Ap. J.*, **254**, 676.  
 Koester, D. 1980, *Astr. Ap. Suppl.*, **39**, 401.  
 Kopal, Z. 1978, in *Dynamics of Close Binary Systems* (Dordrecht: Reidel), p. 329.  
 Latham, D. 1979, in *The MMT and the Future of Ground-Based Astronomy*, ed. T. Weekes (*Smithsonian Ap. Obs. Spec. Rept.* No. 385), p. 119.  
 Liebert, J. 1977, *Ap. J.*, **214**, 446.  
 Liebert, J., Wesemael, F., Hansen, C. J., Fontaine, G., Shipman, H. L., Sion, E. M., Winget, D. E., and Green, R. F. 1986, *Ap. J.*, **309**, 230.  
 Lynden-Bell, D. 1969, *Nature*, **223**, 690.  
 Mayo, S. K., Wickramasinghe, D. T., and Whelan, J. A. J. 1980, in *IAU Colloquium 46, Changing Trends in Variable Star Research*, ed. F. M. Bateson, J. Smak, and I. J. Urch (Waikato, New Zealand: University of Waikato), p. 52.  
 Nather, R. E. 1973, *Vistas Astr.*, **15**, 91.  
 ———. 1984, in *Proc. of the NATO Advanced Study Institute on Cataclysmic Variable Stars*, ed. P. Eggleton and J. E. Pringle (Dordrecht: Reidel), p. 349.  
 Nather, R. E., Robinson, E. L., and Stover, R. J. 1981, *Ap. J.*, **244**, 269.  
 Nather, R. E., Wood, M. A., Winget, D. E., and Liebert, J. 1984, *IAU Circ.*, **4021**.  
 Patterson, J., Nather, R. E., Robinson, E. L., and Handler, F. 1979, *Ap. J.*, **232**, 819.  
 Robinson, E. L. 1979, in *IAU Colloquium 53, White Dwarfs and Variable Degenerate Stars*, ed. H. M. Van Horn and V. Weidemann (Rochester, N.Y.: University of Rochester), p. 343.  
 Robinson, E. L., and Faulkner 1975, *Ap. J. (Letters)*, **200**, L23.  
 Rybski, P. M., Mitchell, A. L., and Montemayor, T. 1977, *Pub. A.S.P.*, **89**, 621.  
 Shafter, A. W., and Szkody, P. 1984, *Ap. J.*, **276**, 305.  
 Smak, J. 1983, *Acta Astr.*, **33**, 333.  
 Solheim, J.-E., Robinson, E. L., Nather, R. E., and Kepler, S. O. 1984, *Astr. Ap.*, **135**, 1.  
 Tull, R. G., Vogt, S. S., and Kelton, P. W. 1979, in *Instrumentation in Astronomy III (Proc. SPIE, Vol. 172, ed. D. Crawford)* (Bellingham, WA: SPIE), p. 90.  
 Vogt, N. 1980, *Astr. Ap.*, **88**, 66.  
 Wegner, G. 1983, *A.J.*, **88**, 1034.  
 Wesemael, F. 1981, *Ap. J. Suppl.*, **45**, 177.  
 Whipple, F. L. 1947, *Harvard Reprint Series*, No. II-19.

FREDERIC V. HESSMAN: Max-Planck-Institut für Astronomie, Königstuhl, D-6900 Heidelberg, Federal Republic of Germany

DONALD W. KURTZ: Department of Astronomy, University of Cape Town, Rondebosch 7700, Cape, South Africa

JAMES W. LIEBERT: Steward Observatory, University of Arizona, Tucson, AZ 85721

R. EDWARD NATHER, DONALD E. WINGET, and MATT A. WOOD: Department of Astronomy, University of Texas, Austin, TX 78712

GARY WEGNER: Department of Physics and Astronomy, Dartmouth College Wilder Laboratory, Hanover, NH 03755

F. WESEMAEL, Département de Physique, Université de Montréal, C.P. 6128, Succ. A., Montréal, Québec, Canada H3C 3J7